Synthesis, structures, spectroscopy and antimicrobial properties of complexes of copper(II) with salicylaldehyde N-substituted thiosemicarbazones and 2,2′-bipyridine or 1,10-phenan...

ARTICLE *in* EUROPEAN JOURNAL OF MEDICINAL CHEMISTRY · APRIL 2014

Impact Factor: 3.45 · DOI: 10.1016/j.ejmech.2014.02.009

6 AUTHORS, INCLUDING:

Harpreet Kaur
O.P. Jindal Global University
37 PUBLICATIONS **113** CITATIONS
SEE PROFILE

Daljit Singh Arora
Guru Nanak Dev University
77 PUBLICATIONS **1,590** CITATIONS
SEE PROFILE

Jerry P. Jasinski
Keene State College
639 PUBLICATIONS **2,502** CITATIONS
SEE PROFILE

European Journal of Medicinal Chemistry 76 (2014) 145–154

Contents lists available at ScienceDirect

European Journal of Medicinal Chemistry

journal homepage: http://www.elsevier.com/locate/ejmech

Original article

Synthesis, structures, spectroscopy and antimicrobial properties of complexes of copper(II) with salicylaldehyde N-substituted thiosemicarbazones and 2,2′-bipyridine or 1,10-phenanthroline

Tarlok S. Lobana [a,*], Shikha Indoria [a], Amanpreet Kaur Jassal [a], Harpreet Kaur [b], Daljit S. Arora [b], Jerry P. Jasinski [c]

[a] Department of Chemistry, Guru Nanak Dev University, Amritsar 143 005, India
[b] Department of Microbiology, Guru Nanak Dev University, Amritsar 143 005, India
[c] Department of Chemistry, Keene State College, Keene, NH 03435, USA

ARTICLE INFO

Article history:
Received 26 July 2013
Received in revised form
6 February 2014
Accepted 7 February 2014
Available online 8 February 2014

Keywords:
Copper(II)
2, 2′-Bipyridine
1,10-Phenanthroline
Salicylaldehyde thiosemicarbazones
Fluorescence
Biological activity

ABSTRACT

Among the biometals (Cu, Co, Ni-cofactors in many enzymes), copper derivatives of O, N, S-donor salicylaldehyde thiosemicarbazones have received considerable attention owing to their potential biological applications. Eight new complexes of salicylaldehyde-N-substituted thiosemicarbazones [5-MeO-2-HO–C_6H_4–C^2(H)=N^3–N^2H–C^1(=S)–N^1H*R*; R = Me, H_2L^1; Et, H_2L^1, Ph, H_2L^3, H, H_2L^4] with copper(II), namely, [Cu(κ^3-O,N,S-L)(κ^2-N,N-L′)] {$(L)^{2-}$ = $(L^1)^{2-}$, L′ = bipy, **1**, phen, **2**; $(L)^{2-}$ = $(L^2)^{2-}$, L′ = bipy, **3**, phen, **4**; $(L)^{2-}$ = $(L^3)^{2-}$, L′ = bipy, **5**, phen, **6**; $(L)^{2-}$ = $(L^4)^{2-}$, L′ = bipy, **7**, phen, **8**} have been isolated. Complexes have slightly distorted square pyramidal geometry around the metal center (τ parameter = 0.243–0.357) and display weak to intense fluorescence in the region, 375–475 nm. These copper complexes have shown significant growth inhibitory activity (antimicrobial activity) against *Staphylococcus aureus* (MTCC740), methicillin resistant *Staphylococcus aureus* (MRSA), *Klebsiella pneumoniae* 1 (MTCC109), *Shigella flexneri* (MTCC1457), *Pseudomonas aeruginosa* (MTCC741) and *Candida albicans* (MTCC227). The activity against MRSA is an interesting observation as the commercially available gentamycin is found to be inactive against this bacterial strain. Specifically complex **5** formed by 5-methoxysalicylaldehyde-N-phenylthiosemicatbazone has shown novel antimicrobial activity against various bacteria and yeast investigated.

1. Introduction

Thiosemicarbazones represent an interesting class of thio-ligands which have shown coordination to metals through different donor atoms forming a variety of complexes with different nuclearities [1]. In addition this class of thio-ligands/their complexes have also shown important biological properties (antitumor, antibiotic, antiviral), in vitro molecular imaging, metal-sensing properties, catalytic and analytical applications [1–6]. In particular salicylaldehyde thiosemicarbazones, $R^1R^2C^2$=N^3–N^2(H)–C(S)–NR^3R^4 (Chart 1, H_2L) constitute an important class of organic molecules whose coordination chemistry with metals has received considerable attention [1,2]. There is special interest in copper(II)-thiosemicarbazone chemistry due to the biological applications of complexes which can be attributed to the possibility of change in its coordination number/oxidation state [7–22]. The thio-ligands have shown coordination to Cu^{II} as monoanions (HL^-, the deprotonation of –OH group) [7–11,22], or as dianions (L^{2-}, the deprotonation of –OH and -N^2H groups) [7–9,12–22], and the geometry around Cu^{II} center is distorted square planar or distorted trigonal bipyramidal in mono- and di-nuclear complexes [7–22]. Several investigations pertain to the R^1 group with no ring substitution (R, R = H, H, Chart 1) and with R^2 = H, while substitution at N^1 atom is varied [7,8,10,12–14,16,22]. There are a few reports with R^2 = Me and with R^1 having no ring substitution (R, R = H, H, Chart 1) [15,18,19]. Further with R^2 = Me and R^1 ring having methyl substitution at 5-position, a phenoxy bridged dimer is reported [20]. For R^2 = H and with substitution at 5 position of R^1 ring (5-NO_2, 5-Cl, 5-Br, 5-CH_3, 5-MeO, Chart 1), only one complex (5-NO_2) is structurally characterized [17]. 5-Bromo-salicylaldehyde-2-methyl thiosemicarbazone, a related thio-ligand, also formed a square planar complex [23]. Finally for R^2 = H and with double substitution of R^1 ring (R, R; Cl, Cl; Br, Br; 3,5-^{t}Bu; 3-MeO, 5-Ph-N=N–, Chart 1)

* Corresponding author.
E-mail addresses: tslasr@gmail.com, tarlokslobana@yahoo.co.in (T.S. Lobana).

http://dx.doi.org/10.1016/j.ejmech.2014.02.009
0223-5234/

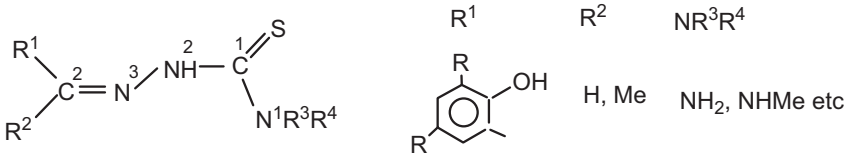

Chart 1. Salicylaldehyde thiosemicarbazones, H_2L.

[9,11,13] distorted trigonal bipyramidal complexes have been reported [13].

Copper(II) complexes reported in literature have shown activities such as antimicrobial [9,12,15,19,21], antitumor [10,11], photoinduced DNA cleavage [14] and oxidation of ascorbic acid in the presence of oxygen [13]. The CuN_3OS core of complexes model the ascorbate oxidation property of dopamine β-hydroxylase (DβH) and peptidylglycine α-hydroxylating monooxygenases (PHM) [13]. Dinuclear complexes have shown little or no antimicrobial activity [19,21]. It is noted that the nature of the substituents in the R^1 ring and the presence of co-ligands both have shown effect on the biochemical properties of complexes [9–15,19,21]. Further, five coordinated complexes with polypyridyl heterocyclic bases as co-ligands showed enhanced antimicrobial activity due to the increase of lipophilicity [12–15]. The studies described in literature pertain to the biological activity either when complexes do not generally have co-ligands [9–11,19,21], or when R^1 ring has no substitution but metal is coordinated to the polypyridyl bases [12–15].

It is noted from above that there is no systematic approach to synthesize new compounds and hence to explore their biological properties. It was thus considered important to adopt a systematic approach and study the effect of substituents in the R^1 ring, employ various heterocyclic bases such as polypyridyls or related ligands and also change substituents at N^1 atom of thiosemicarbazones. Owing to our interest in the chemistry of thiosemicarbazones with transition metals [24–27], it was designed to react copper(II) with salicylaldehyde N-substituted thiosemicarbazones as shown in Chart 2 (H_2L^1, H_2L^2, H_2L^3, H_2L^4) having methoxy substitution at 5-position as well as variable substitution at N^1 atom. The 2,2′-bipyridyl and 1,10-phenanthroline were planned as co-ligands in this investigation. Synthesis, structures, spectroscopy, fluorescence and antimicrobial aspects of complexes are investigated.

2. Results and discussion

2.1. Synthesis, IR spectroscopy and magnetism

Scheme 1 shows the formation of complexes **1**–**8** incorporating 5-methoxy-salicylaldehyde-N-substituted thiosemicarbazones with bipy or phen as co-ligands. In a typical example, $Cu(OAc)_2$ when reacted with H_2L^1 thio-ligand in methanol formed a brown compound of empirical composition, [Cu(O,N^3,S-L^1)]. The addition of bipy to the solid [Cu(O, N^3, S-L^1)] suspended in acetonitrile–methanol mixture led to the formation of a dark green complex of stoichiometry, [Cu(O,N^3,S-L^1)(N,N-bipy)]·CH_3OH (**1**). Other thio-ligands, namely, H_2L^2, H_2L^3, H_2L^4 also yielded complexes of similar stoichiometry, [Cu(O,N^3,S-L)(N, N-bipy)] (L = L^2, **3**; L^3, **5**; L^4, **7**), [Cu(O,N^3,S-L)(N,N-phen)D] (L = L^1, D = 0.5H_2O **2**; [Cu(O,N^3,S-L)(N,N-phen)] (L^2 **4**, L^3,**6**; L^4, **8**). The complexes are dark green in color and are soluble in dichloromethane, methanol, acetonitrile and dimethyl sulfoxide.

The IR spectrum of H_2L^2 ligand shows ν(N^1–H) band at 3344 cm^{-1} which appears at 3341 cm^{-1} in its complex, [CuL^2(bipy)] **3**. A broad band of the free ligand due to ν(N^2–H) and ν(O–H) occurred at 3238 cm^{-1}, which disappeared in the complex suggested deprotonation of both (N^2–H) and (O–H) moieties and the ligand binding to the metal as a dianion. Complex **4** with the same ligand H_2L^2 showed similar IR spectral changes corresponding to the ν(N^1–H), ν(N^2–H) and ν(O–H) stretching frequencies. In the IR spectrum of free H_2L^4, the bands due to ν(N^1–H_2), ν(N^2–H) and ν(O–H) occur at 3379 s, 3280 m and 3249 s(b) cm^{-1} respectively but in complex **7**, only $-N^1H_2$ group showed bands at 3346 m, 3281 m cm^{-1}. Similar behavior is noticed in complex **8**. As above, the IR bands of free ligand, H_2L^3 due to ν(N^2–H) and ν(O–H) at 3396 cm^{-1} (br) disappeared in complexes **5** and **6**. Complexes **1** and **2** showed similar behavior. The ν(O–H) bands of CH_3OH and H_2O appeared at same position, 3380 cm^{-1} supporting their presence in complexes **1** and **2**. The diagnostic ν(C–S) bands of free ligands lie in the region, 1027–1031 cm^{-1} which shifted to the range, 813–815 cm^{-1} in complexes (see Experimental/supplementarty for more details). The magnetic moments of complexes [μ_{eff} = 1.79 (**1**), 1.94 (**2, 8**), 1.80 (**3**), 2.12 (**4**), 2.08 (**5**), 1.97 (**6**), 1.81(7) BM] suggest the presence of Cu^{II} oxidation state in complexes.

2.2. Crystal and molecular structure

The crystals of complexes **1**–**5, 7** and **8** were grown from CH_2Cl_2–MeOH or CH_3CN–MeOH mixtures. Complex **6** though crystalline did not yield crystals of size suitable for X-ray crystallography, however, the analytical data supported stoichiometry similar to that of other complexes. Complexes **1**, **4** and **5** formed orthorhombic crystals, **3** and **7** formed triclinic crystals and **2** and **8** formed monoclinic crystals in space groups $Pna2_1$ (**1**), $Pna2_1$ (**4**), Pbca (**5**), P-1 (**3**), $P2_1/c$ (**2, 7**) and $P2_1/n$ (**8**) respectively (Table 1). Complexes **1**–**8** are mononuclear in which the metal is bonded to a thiosemicarbazone through its O, N, S-donor atoms and N,N-donor atoms of bipy or phen heterocyclic bases. The O, N, S-donor atoms occupy the basal plane and the heterocyclic N,N-bases occupy the axial-equatorial sites.

The bipyridine complexes, **1, 3, 5** and **7** have Me, Et, Ph or H groups at N^1 atom. The molecular structure of complex **1** is shown in Fig. 1. Copper atom is coordinated by phenolato oxygen (O1), azomethine nitrogen (N1), thiolato sulfur (S), and bipyridine nitrogen atoms, N(4) and N(5). The atoms O(1), N(1), S(1) (thio-ligand), and N(4) (bipy ligand) occupy square basal plane while N(5) (bipy) occupies the axial position. The τ parameter of 0.3 suggests that the geometry of complex is distorted square-pyramidal. Complexes **3**, **5** and **7** have similar structures (Figs. 3,

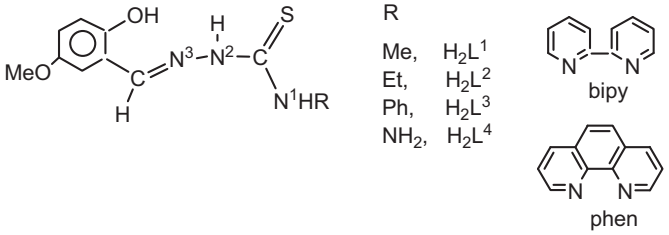

Chart 2. Thiosemicarbazones and co-ligands.

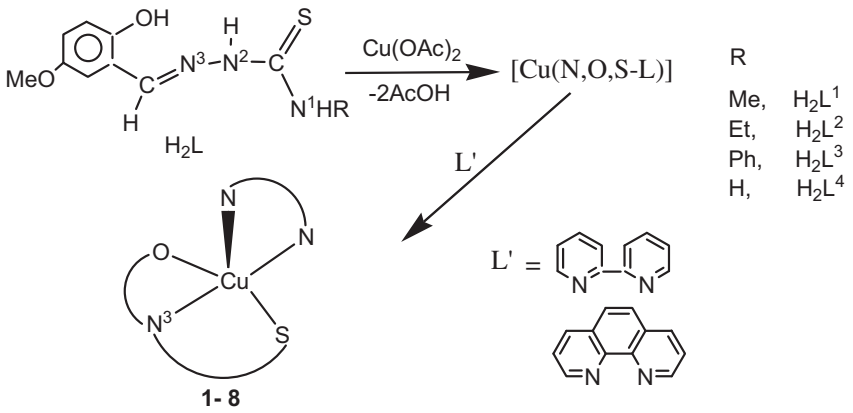

Scheme 1. Synthetic route to complexes.

5 and 6 respectively). The bond lengths and bond angles of all these complexes are similar with minor differences as shown in Table 2. The molecular geometry is close to a square pyramid. The τ parameters vary in the close range, 0.260–0.357. The distortion from a square pyramid varies in the order R = Ph (**5**) > Me(**1**) > Et(**3**) > H(**7**). The Cu–N_{eq}(bipy) distances are shorter than the Cu–N_{ax}(bipy) bond distances. Further Cu–$N_{(thio\text{-}ligand)}$ bond distance is shorter than the Cu–$N_{eq(bipy)}$ bond distance. The trans O–Cu–S bond angles deviate significantly from 180°, while N–Cu–N_{eq} angles are close to 180°. The N_{ax}–Cu–N_{eq} bite angles are shortest and similar.

The 1,10-phenanthroline complexes, **2, 4** and **8** have Me, Et and H groups at N^1 atom. Complex **2** showed the presence of two independent molecules in the unit cell. In molecule **2a,** copper atom is coordinated by phenolato oxygen (O1), azomethine nitrogen (N5), thiolato sulfur (S), and phen nitrogen atoms, N(2) and N(5). The atoms O(1), N(5), $S(1)_{(thio\text{-}ligand),}$ and $N(1)_{(phen\ ligand)}$ occupy square basal plane, while $N(2)_{(phen)}$ occupies the axial position (Fig 2). The τ parameter of 0.34 suggests that the geometry of complex is distorted square-pyramidal. Similarly, the τ value for complex **2b** is 0.24 which suggests more distortion from square pyramid of **2a** molecule than that of **2b** molecule. The molecular structure and bond parameters of **4** and **8** (Figs. 4 and 7) are similar to those of complex **2**. The τ values vary in the range, 0.243 to 0.341. The structures as well as bond parameters are also similar to those of bipy complexes. The coordination pattern and bonding trends are similar to those reported in literature [13]. Methanol in **1** and **4** as well as H_2O in **2** was lying in the lattice as non-bonded.

2.3. ESI-mass, electronic absorption and fluorescence spectroscopy

ESI-mass spectral study has shown an intense molecular ion for each of complexes **1**, **2**, **3**, **4**, **6** and **7**. It reveals the stability of complexes under ESI-mass environments. This ionization may be represented as follows:

$$\left[Cu\left(\kappa^3-O,N,S-L\right)\left(\kappa^2-N,N-L\prime\right)\right] \rightarrow \left[Cu\left(\kappa^3-O,N,S-L\right)\left(\kappa^2-N,N-L\prime\right)\right]^+$$

$$L = \left(L^1\right)^{2-},\quad L\prime = \text{bipy } \mathbf{1};\left(L^1\right)^{2-},\quad L\prime = \text{phen } \mathbf{2}$$

$$L = \left(L^2\right)^{2-},\quad L\prime = \text{bipy } \mathbf{3};\left(L^2\right)^{2-},\quad L\prime = \text{phen } \mathbf{4}$$

$$L = \left(L^3\right)^{2-},\quad L\prime = \text{phen } \mathbf{6};\left(L^4\right)^{2-},\quad L\prime = \text{bipy } \mathbf{7}$$

The electronic absorption spectral data and fluorescence spectral data of complexes are listed in the experimental section. For observing d–d transitions based on Cu^{II} ion, 10^{-3} M solutions were used and for transitions centered on the ligands and involving charge transfer (CT) bands, the 10^{-4}–10^{-5} M solutions were used. The absorption spectral bands can be classified into four categories. The electronic spectral bands in the region, 265–295 nm are assigned to $\pi \rightarrow \pi^*$ transitions, and those in the region 305–347 nm are assigned to $n \rightarrow \pi^*$ plus $S \rightarrow Cu$ transitions. The bands in the region 389–430 nm are attributed to the combined $O \rightarrow Cu$ (CT) and $^2B_1$–^2E_g [ν_3 (d–d)] transitions. Finally, the bands in the region 560–585 nm are pure d–d (ν_3) transitions. The d–d transitions confirm divalent oxidation state of the metal in complexes **1**–**8** [16].

As regards fluorescence spectral studies, all complexes were screened for fluorescence corresponding to the excitation wavelength of 355 nm. However, complexes **1**, **3** and **7** were non-fluorescent and other complexes, namely, **2**, **4**–**6** and **8,** most of which have phen as co-ligand were found to be fluorescent in the region, 375–475 nm (Fig 8). It can be noted that complex **4** with N-ethyl substitution at C^1 carbon has shown the most intense emission bands covering a wide visible region of the spectrum. Complex **5** has shown similar emission behavior, though emission intensity is somewhat less than that shown by complex **4** and likewise emission intensity of complexes **2 a**nd **8** is lowest. Finally, complex **6** has shown one emission band at $\lambda = 400$ nm with a vibrational fine structure at $\lambda = 380$ nm. The origin of fluorescence emission is attributed to π–π^* transitions centered on phen/bipy ligands.

2.4. Antimicrobial studies

2.4.1. Importance of this study

The antimicrobial investigations have been carried out against gram negative bacteria, namely, *Klebsiella pneumoniae* 1 (MTCC109), *Shigella flexneri* (MTCC1457), *Pseudomonas aeruginosa* (MTCC741), gram positive bacteria, namely, *Staphylococcus aureus* (MTCC740) and methicillin resistant *Staphylococcus aureus* (MRSA) and one yeast, *Candida albicans* (MTCC227. These bacteria are responsible for causing gastrointestinal tract infections and respiratory infections. It is known that *K. pneumoniae* 1 (MTCC109), *P. aeruginosa* (MTCC741) and *S. flexneri* (MTCC1457) acquire resistance more readily due to their outer membrane which contains narrow porin channels, a lipopolysaccharide moiety responsible to

Table 1
Crystallographic data for complexes **1**–**5, 7, 8**.

	1	**2**	**3**	**4**
Empirical formula	$C_{20}H_{19}CuN_5O_2S{\cdot}CH_3OH$	$C_{22}H_{19}CuN_5O_2S.0.5H_2O$	$C_{21}H_{21}CuN_5O_2S$	$C_{23}H_{22}CuN_5O_2S{\cdot}CH_3OH$
M	489.04	490.03	471.05	528.12
T(K)	293(2)	295(2)	296(2)	296(2)
Crystal system	Orthorhombic	Monoclinic	Triclinic	Orthorhombic
Space group	$Pna2_1$	$P2_1/c$	P-1	$Pna2_1$
Unit cell dimensions				
a(Å)	18.1670(3)	10.8253(4)	8.290(3)	20.100(2)
b(Å)	6.6879(2)	12.3099(5)	10.380(5)	6.801(1)
c(Å)	17.3213(3)	32.1284(11)	13.2628(2)	17.339(2)
α(°)	90.00	90.00	71.647(2)	90.00
β(°)	90.00	97.928(2)	82.728(2)	90.00
γ(°)	90.00	90.00	75.73(2)	90.00
V(Å^3)	2104.5(8)	4240.5(3)	1049.48(8)	2370.0(4)
Z	4	4	2	4
D_{calcd}(g cm^{-3})	1.543	1.535	1.491	1.480
μ(mm^{-1})	1.171	1.162	1.168	1.046
F(000)	1012	2016	486	1096
Reflections collected	22893	34143	27283	12529
Unique reflections	6598, (R_{int} = 0.0308)	9213, (R_{int} = 0.0547)	7564, (R_{int} = 0.0244)	4392, (R_{int} = 0.0435)
Data/restraints/parameters	6598/1/287	9213/5/602	7564/1/276	4392/2/311
Reflens.with [I > 2σ(I)]	6152	5924	5487	3570
R indices				
R_1	0.0281	0.0477	0.0478	0.0346
WR_2	0.0646	0.1120	0.1282	0.0795
R indices (all data)				
R_1	0.0317	0.0899	0.0724	0.0483
WR_2	0.0665	0.1315	0.1474	0.0864
Largest diff. Peak and hole	0.400 and −0.311 e Å^{-3}	1.407 and −0.308 e Å^{-3}	1.759 and −0.525 e Å^{-3}	0.397 and −0.388 e Å^{-3}

	5	**7**	**8**
Empirical formula	$C_{25}H_{21}CuN_5O_2S$	$C_{19}H_{17}CuN_5O_2S$	$C_{21}H_{17}CuN_5O_2S$
M	519.07	443.00	467.02
T(K)	173(2)	296(2)	296(2)
Crystal system	Orthorhombic	Triclinic	Monoclinic
Space group	Pbca	$P2_1/c$	$P2_1/n$
Unit cell dimensions			
a(Å)	13.8291(4)	16.359(2)	16.278(2)
b(Å)	9.5928(4)	6.786(1)	6.906(1)
c(Å)	34.298(13)	18.209(2)	19.445(3)
α(°)	90.00	90.00	90.00
β(°)	90.00	110.607(5)	112.95(1)
γ(°)	90.00	90.00	90.00
V(Å^3)	4549.9(3)	1892.1(4)	2013.1(5)
Z	8	4	4
D_{calcd}(g cm^{-3})	1.516	1.555	1.541
μ(mm^{-1})	2.492	1.290	1.217
F(000)	2136	908	956
Reflections collected	33005	15528	13622
Unique reflections	4348, (R_{int} = 0.0505)	2645, (R_{int} = 0.0598)	3658, (R_{int} = 0.0810)
Data/restraints/parameters	4348/0/309	2645/0/254	3658/2/278
Reflens.with [I > 2σ(I)]	3942	4097	2185
R indices			
R_1	0.0332	0.0473	0.0518
WR_2	0.0916	0.1003	0.0878
R indices (all data)			
R_1	0.0369	0.0887	0.1090
WR_2	0.0949	0.1163	0.1056
Largest diff. Peak and hole	0.341 and −0.427 e Å^{-3}	0.343 and −0.287 e Å^{-3}	0.340 and −0.331 e Å^{-3}

slow down the transmembrane diffusion of lipophilic antibiotics [28]. It is also important to highlight that methicillin-resistant *Staphylococcus aureus* (MRSA) causes nosocomial and community-onset infections which have shown increasing endemic and epidemic spread in the last four decades, while its control has become a serious concern worldwide [29–33]. The control and prevention of MRSA cross-infection is among the most important challenges of infection control, especially due to the fact that these bacteria have shown resistance not only to methicillin but also to several other drugs except vancomycin (glycopeptides) [34–36]. The increased resistance has invited the search for new antimicrobial agents, a challenging task for chemists [37,38].

2.4.2. Biological data and discussion of results

The antimicrobial activities of mixed-ligand complexes, [Cu(κ^3-O,N,S-L)(N,N-donor)] **1**–**8** (Class I compounds), [Cu(κ^3-O,N,S-L)]$_n$ compounds without bipyridine or phenanthroline bases (Class II compounds) and thio-ligands H_2L {H_2L = H_2L^1, H_2L^2, H_2L^3, H_2L^4} (Class III compounds) have been studied in dimethyl sulfoxide (dmso). The biological data listed in Table 3 reveal that, in general,

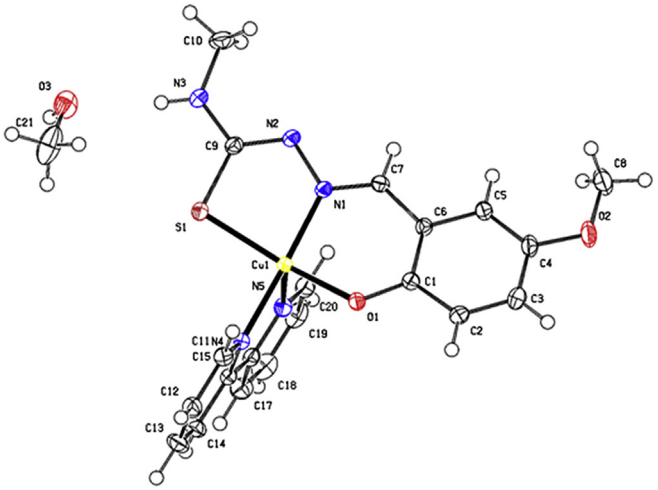

Fig. 1. Molecular structure of complex [Cu(κ^3-O,N,S-L^1)(κ^2-N,N-bipy)]·CH_3OH (**1**).

the antimicrobial activity of three types of compounds varies in the order : Class I > Class II > Class III. Thus the mixed-ligand complexes become the preferred choice for antimicrobial activity and some most significant observations made are presented as follows. Complexes **1**–**5** and **8** have shown highest antimicrobial activity ranging from 25 to 32 mm zone of inhibition (zoi) against methicillin resistant *staphylococcus aureus* (MRSA). This is an interesting observation as the commercially available *Gentamycin* is found to be inactive against this bacterial strain. Complexes **1**, **3**, **5**, **7** and **8** have shown activity against *S. aureus* (23–27 mm zoi) which is comparable to that of *Gentamycin* (25 mm zoi) (Table 3). Complexes **1**–**8** have shown activity against *K. pneumoniae* 1 in 23–33 mm zoi and it is interesting to remark that complexes **2** and **4** showed activity (30–33 mm zoi) close to that of *Gentamycin* (32 mm zoi). None of Class II compounds were active against *S. flexneri*, two compounds of Class III were active but activity is much lower than that shown by complexes **4**–**8** (15–18 mm zoi), which is comparable to that of *Gentamycin* (20 mm zoi). As regards activity against *P. aeruginosa* only complex **5** and two of Class II compounds showed

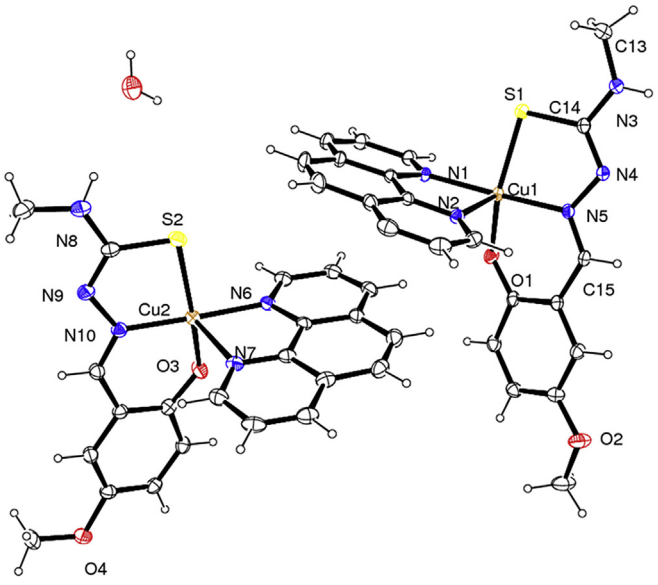

Fig. 2. Molecular structure of complex [Cu(κ^3-O,N,S-L^1)(κ^2-N,N-phen)]·$0.5H_2O$ (**2**).

activity, but activity of complex **5** was as good as that of *Gentamycin*. All complexes showed activity against *C. albicans* in the range 23–31 mm zoi and activity of complex **1** (31 mm zoi) was as good as that of commercial *Amphotericin* (34 mm zoi). From the above discussion it is noted that among bipyridyl complexes, complex **5** with a phenyl substituent at N^1 atom of H_2L^3 ligand appears generally suitable for inhibiting all the microorganisms including the methicillin resistant *Staphylococcus aureus* and it can be considered as a potential antimicrobial agent.

It can be seen from Table 4 that several complexes were active at minimum inhibitory concentration (MIC) of **5** μg/mL (methicillin resistant *Staphylococcus aureus*: **4, 5, 8**; *K. pneumoniae 1*: **4**, **5**, **7**; *C. albicans*: **1**–**4**), MIC of 10 μg/mL (methicillin resistant *Staphylococcus aureus*: **1**–**3**; *S. aureus*: **1**, **3**, **5**, **7, 8**; *K. pneumoniae 1*: **1**, **2**, **6**, **8**; *C. albicans*: **5**–**8**), MIC of 25 μg/mL (methicillin resistant *staphylococcus aureus*: **6, 7**; *S. aureus*: **2, 4, 6**; *K. pneumoniae 1*: **3**). Complexes **6** and **8** showed activity at MIC of 750 μg/mL for *S. flexneri* while only complex **5** showed activity at MIC of 750 μg/mL for *P. aeruginosa*. Further it has been observed that bipyridyl and phenanthroline base adducts of copper(II) complexes with thiosemicarbazones are less toxic in biological systems than the free thio-ligand. Higher antimicrobial activity of complexes is attributed to their better membrane penetrating ability and the cause of inhibitory action of complexes can be due to their interaction with enzyme prosthetic group which inhibits the replication of DNA [39].

2.4.3. A comparison with literature reports of relevance to the present study

It is pertinent to point out here that in literature reports with 3-methoxy substitution along with 5-phenylazo moiety in the 2-hydroxy phenyl ring (Chart 1) and with both hydrogens at N^1 atom (-ie, $-N^1H_2$), complexes were dinuclear in the absence of co-ligands and were found to show antitumor activity, though no antimicrobial activity was studied [11]. With 5-methoxy substitution along with methyl/ethyl substitution at N^1 nitrogen of the thio-ligand in the absence of co-ligands again formed dinuclear complexes which did not show antimicrobial activity [21]. The presence of 5-methoxy substitution in the 2-hydroxy phenyl ring and with hydrogen, methyl, ethyl and phenyl substituents at N^1 atom, five coordinate complexes **1**–**8** have been prepared using bipyridine/phenanthroline as co-ligands which have shown unusual antimicrobial activity as detailed above. This activity could be attributed to the fact that five coordinate complexes exhibit greater lipophilicity than four coordinate dinuclear complexes [11,21]. The fact that several Class II compounds have shown significant activity suggests that the nature of the thio-ligand with different substituents at N^1 atom appears to be important. Further increase in activity shown by mixed-ligand Class I compounds suggests a cumulative effect of thio-ligands and N,N-donor bases bonded to Cu^{II} metal center which determine the total antimicrobial activity. Complex **5** formed by 5-methoxysalicylaldehyde-N-phenylthiosemicatbazone has shown novel antimicrobial activity against various bacteria and fungi investigated.

3. Conclusion

In the present study salicylaldehyde-N substituted thiosemicarbazones having 5-methoxy substitution in the 2-hydroxy phenyl ring along with different substituents at N^1 nitrogen using 2,2′-bipyridine and 1,10-phenanthroline as co-ligands formed distorted square pyramidal complexes which have shown significant growth inhibitory activity against *S. aureus* (MTCC740), methicillin resistant *Staphylococcus aureus* (MRSA), *K. pneumoniae* 1 (MTCC109), *S. flexneri* (MTCC1457), *P. aeruginosa* (MTCC741) and *C.*

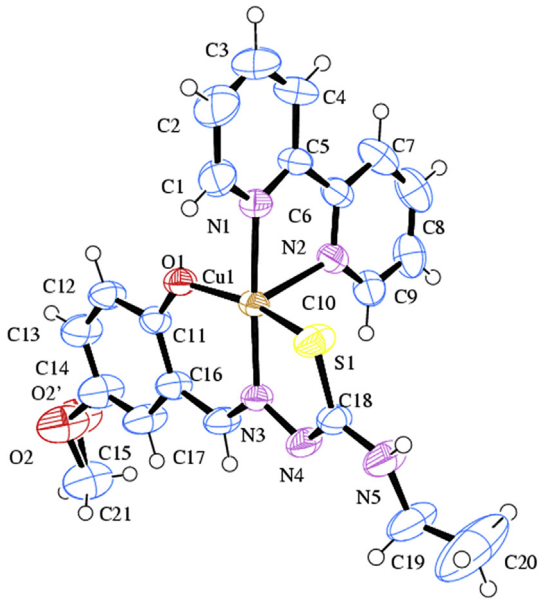

Fig. 3. Molecular structure of complex [Cu(κ^3-O,N,S-L^2)(κ^2-N,N-bipy)] **(3).**

albicans (MTCC227). Complex **5** formed by 5-methoxysalicylaldehyde-N-phenylthiosemicarbazone has shown novel antimicrobial activity against various bacteria and fungi investigated. The results are encouraging especially related to MRSA and further pursuit is needed both in alteration of groups in rings at C^2 carbon, at N^1 atoms of thiosemicarbazones and the nature of co-ligands. The activity against MRSA is an interesting observation as the commercially available gentamycin is found to be inactive against this bacterial strain.

4. Experimental section

4.1. Materials and methods

Copper(II) acetate monohydrate $Cu(OAc)_2 \cdot H_2O$, thiosemicarbazide, N-methyl thiosemicarbazide, N-ethyl thiosemicarbazide, N-phenyl thiosemicarbazide, 5-methoxysalicylaldehyde, 2,2-bipyridine (bipy) and 1,10-phenanthroline (phen) were procured from Aldrich Sigma Ltd. The thio ligands were synthesized by conventional procedures [25,40]. Elemental analysis C, H, and N were carried out with a thermoelectron FLASHEA1112 analyzer. The melting points were determined with a Gallenkamp electrically heated apparatus. Magnetic susceptibility measurements were made at room temperature with the help of a magnetic susceptibility balance procured from Johnson Matthey, Catalytic Systems Division Equipment, UK. The IR spectra of compounds were recorded in 4000–450 cm^{-1} region with a Perkin Elmer FT-IR Spectrometer by making their KBr pellets. The UV–visible spectra of compounds were recorded in dmso or methanol solvents with the help of a UV-1601 PC Shimadzu spectrophotometer. Fluorescence spectra of complexes were recorded with a Varian Cary Eclipse Fluorescence spectrophotometer. The mass spectra were recorded using Bruker Daltonik LS-MS high resolution microTOF-Q II 10356.

4.2. Synthesis of complexes

Complexes **1**–**8** were prepared by initially reacting copper(II) acetate with a thio-ligand which formed a compound of empirical composition [Cu^{II}(O,N^3,S-L] (presumably a dimer or an oligomer) which was reacted with a N,N-donor co-ligand. The experimental procedures and characterization data are summarized below.

4.2.1. [Cu(κ^3-O,N,S-L^1)(κ^2-N,N-bipy)]·CH_3OH (**1**)

To a pale yellow solution of thio-ligand L^1H_2 (0.029 g, 0.127 mmol) in methanol (15 mL) was added dark green solid $Cu(OAc)_2 \cdot H_2O$ (0.025 g, 0.125 mmol). Brown precipitate start forming immediately and were stirred for one hour to ensure complete precipitation. The precipitate were filtered and allowed to dry at room temperature. The analytical data supported the formation of a compound of empirical composition, [Cu^{II}(O,N, S-L^1] (Anal. calcd for $C_{10}H_{11}CuN_3O_2S$: C 39.93; H 3.69; N 13.97; Found: C 40.06; H 3.47; N 13.78%, μ_{eff} = 2.01 BM). To a suspension of [Cu^{II}(O,N,S–L^1] (0.028 g, 0.092 mmol) in a mixture of acetonitrile and methanol (1 : 1 v/v) was added solid bipy co-ligand (0.014 g, 0.092 mmol) and the contents were stirred for 15 min. A clear dark green solution formed was allowed to evaporate at room temperature which yielded a dark green complex (Yield. 0.031 g, 71%, M.p. 206–208 °C); μ_{eff} = 1.79 BM. $C_{20}H_{19}CuN_5O_2S \cdot CH_3OH$: Calcd. C 52.56; H 4.19; N 15.32; S 7.02; Found: C 52.32; H 4.04; N 15.17; S 7.12%. IR (KBr, selected absorption bands): ν(N^1–H) 3419 s; ν(O–H)

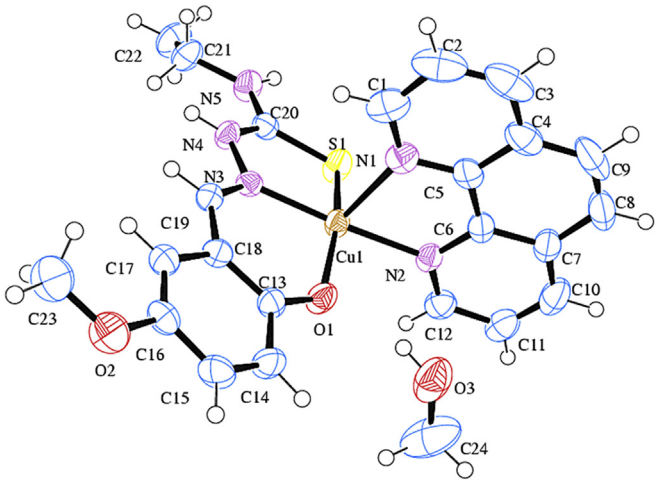

Fig. 4. Molecular structure of complex [Cu(κ^3-O,N,S-L^2)(κ^2-N,N-phen)]·CH_3OH **(4).**

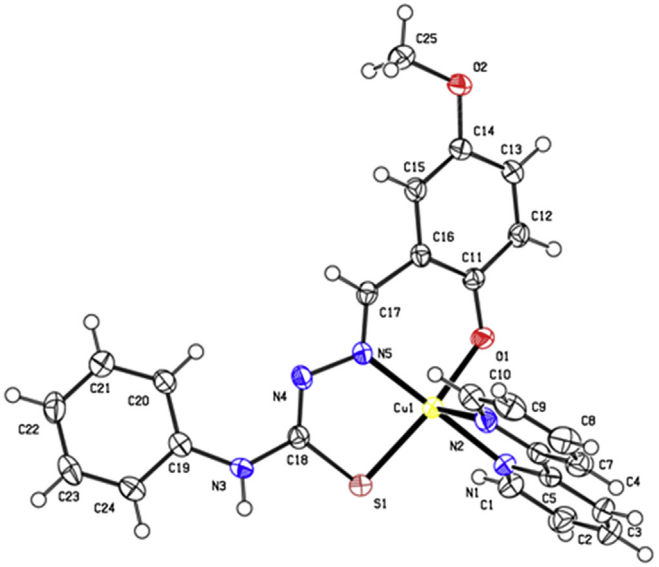

Fig. 5. Molecular structure of complex [Cu(κ^3-O,N,S-L^3)(κ^2-N,N-bipy)] **(5).**

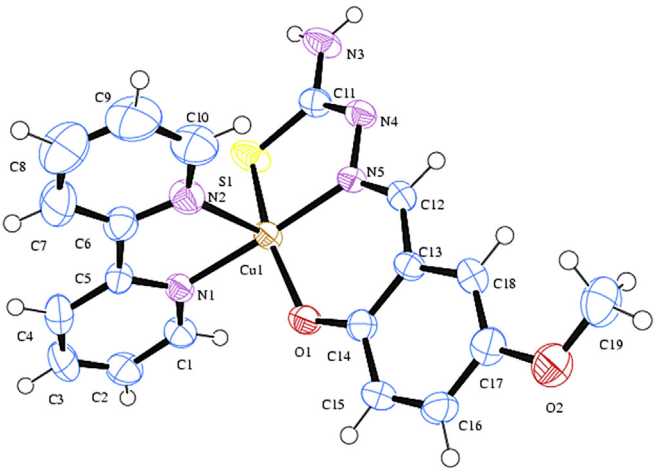

Fig. 6. Molecular structure of complex [Cu(κ^3-O,N,S-L^4)(κ^2-N,N-bipy)] (**7**).

3380 s (CH_3OH), ν(C–H) 3010 w, 2990 w, 2940 w, ν(C–H) 2825 m(CH_3O–); ν(C=N) + ν(C=C) + δ(N–H) 1601 s, 1562 s, 1522 s, 1508 s, δ(C–H) 1484 s; 1440 s, 1407 m; 1272 s, 1190 s, 1158 s, 1048 s, 950 s, ν(C–S) 813 s; 762 s, 736 s, 465 m cm^{-1}. Electronic absorption spectrum, DMSO, λ_{max}/nm, ε/L mol^{-1} cm^{-1}: [10^{-3} M] 565 m, br (2.51×10^2); [10^{-5} M] 420 s, br (1.21×10^4), 330 br (1.96×10^4), 295 m (3.44×10^4). The crystals were grown from dichloromethane–methanol mixture (3:1 v:v) over a period of 10 days. Complexes **2**–**8** were prepared by a similar method. ESI mass data: calcd for $C_{20}H_{19}CuN_5O_2S$, $[M]^+$ 456; obsd. $m/z = 457$ s.

*4.2.2. [Cu(κ^3-O,N,S-L^1)(κ^2-N,N-phen)]·0.5H$_2$O (**2**)*

To a suspension of [Cu^{II}(O,N,S-L^1)] (0.028 g, 0.089 mmol) in a mixture of acetonitrile and methanol (1:1 v/v) was added phen co-ligand (0.018 g, 0.089 mmol) and the contents were stirred for 15 min. A clear dark green solution formed was allowed to evaporate at room temperature which yielded a dark green complex (Yield. 0.032 g, 70%, M.p. 212–214 °C); μ_{eff} = 1.94 BM. $C_{22}H_{19}CuN_5O_2S{\cdot}0.5H_2O$: Calcd. C 53.92; H 4.11; N 14.29; S 6.54; Found: C 54.07; H 3.97; N 14.42; S 6.41%. IR (KBr, selected absorption bands): ν(N^1–H) 3418 s; ν(O–H) 3380 s (H_2O); ν(C–H) 2933 w, 2897 w, 2885 w; ν(C–H) 2833 m(CH_3O–); ν(C=N) + ν(C=C) + δ(N–H) 1592 s, 1567 s, 1507 s; δ(C–H) 1472 s, 1438 s, 1414 m; 1297 s, 1272 s, 1190 s, 1158 s, 1034 s, 950 s, 846 s; ν(C–S) 813 s; 768 s, 727 s, 475 m cm^{-1}. Electronic absorption spectrum, MeOH, λ_{max}/nm, ε/L mol^{-1} cm^{-1}: [10^{-3} M] 575 m, br (1.92×10^2); [10^{-4} M] 404 s, br (8.93×10^3), 321 br (1.64×10^4), 290 m (2.32×10^4), 269 m (3.91×10^4). Fluorescence spectrum: (λ^{em}_{max} = 378, 461 nm; λ^{ex}_{max} = 355 nm). ESI mass data: calcd for $C_{22}H_{19}CuN_5O_2S$, $[M]^+$, $m/z = 480$; obsd. $m/z = 481$ s. n.

*4.2.3. [Cu(κ^3-O,N,S-L^2)(κ^2-N,N-bipy)](**3**)*

To a suspension of [Cu^{II}(O,N,S-L^2)] (0.025 g, 0.079 mmol) in a mixture of acetonitrile and methanol (1:1 v/v) was added bipy co-ligand (0.016 g, 0.079 mmol) and the contents were stirred for 15 min. A clear dark green solution was allowed to evaporate at room temperature, which yielded dark green complex (Yield. 0.03 g, 78%, M.p. 216–218 °C); μ_{eff} = 1.80 B.M. $C_{21}H_{21}CuN_5O_2S$: Calcd. C 53.55; H 4.49; N 14.87; S 6.81; Found: C 53.78; H 4.36; N 14.95; S 6.69%. IR (KBr, selected absorption bands): ν(N^1–H) 3342 br; ν(C–H) 2970 m, 2927 m, 2871 m; ν(C–H) 2830 m (CH_3O–); ν(C=N) + ν(C=C) + δ(N–H) 1589 s, 1538 s; δ(C–H) 1471 s, 1438 s, 1412 s; 1297 s, 1218 s, 1190 s, 1160 s, 1096 s, 1034 s, 1021 s, 937 s, 836 s; ν(C–S) 815 s; 735 s, 649 s, 476 m cm^{-1}. Electronic absorption spectrum, MeOH, λ_{max}/nm, ε/L mol^{-1} cm^{-1}: [10^{-3} M] 570 s, br (1.63×10^2); [10^{-4} M] 404 s, br (6.81×10^3), 320 br (1.24×10^4), 290 m (1.51×10^4), 268 m (2.70×10^4). ESI mass data: calcd for $C_{21}H_{21}CuN_5O_2S$, $[M]^+$, $m/z = 470$; obsd. $m/z = 471$ s.

*4.2.4. [Cu(κ^3-O,N,S-L^2)(κ^2-N,N-phen)]·CH$_3$OH (**4**)*

To a suspension of [Cu^{II}(O,N,S-L^2)] (0.025 g, 0.079 mmol) in a mixture of acetonitrile and methanol (1:1 v/v) was added phen co-ligand (0.012 g, 0.079 mmol) and the contents were stirred for 15 min. A clear dark green solution was allowed to evaporate at room temperature, which yielded dark green complex. (Yield. 0.031 g, 73%, M.p. 227–229 °C); μ_{eff} = 2.12 BM. $C_{23}H_{22}CuN_5O_2S{\cdot}CH_3OH$: Calcd. C 55.69; H 4.47; N 12.81; S 6.46; Found: C 55.72; H 4.37; N 13.08; S 6.29%. IR (KBr, selected absorption bands): ν(N^1–H) 3342 br; ν(C–H) 2970 m, 2925 m, 2873 m; ν(C–H) 2832 m (CH_3O-); ν(C=N) + ν(C=C) + δ(N–H) 1589 s, 1534 s; δ(C–H) 1498 s; 1472 s, 1414 s; 1298 s, 1219 s, 1199 s, 1163 s, 1097 s, 1042 s, 1022 s, 938 s, 836 s; ν(C–S) 815 s; 764 s, 736 s, 650 s, 625 s, 486 m cm^{-1}. Electronic absorption spectrum, MeOH, λ_{max}/nm, ε/L mol^{-1} cm^{-1}: [10^{-3} M] 574 s, br (2.10×10^2); [10^{-4} M] 423 m, br (9.70×10^3), 330 br (1.64×10^4), 297 m (1.52×10^4). Fluorescence spectrum: (λ^{em}_{max} = 400, 456 nm; λ^{ex}_{max} = 355 nm). ESI mass data : calcd for $C_{23}H_{22}CuN_5O_2S$, $[M]^+$, $m/z = 495.5$; obsd. $m/z = 495.3$ s.

*4.2.5. [Cu(κ^3-O,N,S-L^3)(κ^2-N,N-bipy)] (**5**)*

To a suspension of [Cu^{II}(O,N,S-L^3)] (0.03 g, 0.082 mmol) in acetonitrile was added bipy co-ligand (0.013 g, 0.083 mmol) and the contents were stirred for 15 min. The clear dark green solution obtained was allowed to evaporate at room temperature, which yielded dark green crystals. (Yield. 0.043 g, 81%, M.p. 211–213 °C). μ_{eff} = 2.08 BM. $C_{25}H_{21}CuN_5O_2S$: Calcd. C 57.85; H 4.08; N 13.49, S 6.18; Found: C 58.06; H 4.12; N 13.17, S 6.09%. IR (KBr, selected absorption bands): ν(N^1–H) 3418 br; ν(C–H) 2993 m, 2932 m, 2865 m; ν(C–H) 2825 m (CH_3O-); ν(C=N) + ν(C=C) + δ(N–H) 1601 s, 1561 s, 1522 s; δ(C–H) 1485 s, 1440 s, 1407 s, ν 1272 s, 1223 s; 1191 s, 1159 s, 1047 s, 950 s, 854 s; ν(C–S) 814 s; 762 s, 735 s, 468 m cm^{-1}. Electronic absorption spectrum, MeOH, λ_{max}/nm, ε/L mol^{-1} cm^{-1}: [10^{-3} M] 570 br (3.00×10^2); [10^{-4} M] 414 s, br (7.71×10^3), 327 s (1.36×10^4), 287 m (1.43×10^4). Fluorescence spectrum: (λ^{em}_{max} = 400, 470 nm; λ^{ex}_{max} = 355 nm).

*4.2.6. [Cu(κ^3-O,N,S-L^3)(κ^2-N,N-phen)] (**6**)*

To a suspension of [Cu^{II}(O,N,S-L^3)] (0.03 g, 0.083 mmol) in a mixture of acetonitrile and methanol was added phen (0.017 g, 0.083 mmol) and the contents were stirred for 15 min. The clear dark green solution obtained was allowed to evaporate at room temperature, which yielded dark green crystalline complex (Yield. 0.037 g, 82%, M.p. 223–225 °C); μ_{eff} = 1.97 BM. $C_{27}H_{21}CuN_5O_2S$: Calcd. C 59.71; H 3.90; N 12.90; S 5.90; Found: C 59.90; H 3.73; N 13.06; S 5.81%. IR (KBr, selected absorption bands): ν(N^1–H) 3401 br; ν(C–H) 3059 m, 2986 m, 2929 m; ν(C–H) 2830 m (CH_3O–); ν(C=N) + ν(C=C) + δ(N–H) 1583 s, 1535 s, δ(C–H) 1489 s, 1471 s, 1426 s; 1311 s, 1256 s, 1243 s, 1209 s, 1157 s, 1041 s, 950 s, 845 s; ν(C–S) 812 s; 774 s, 755 s, 726 s, 695 s, 509 m cm^{-1}. Electronic absorption spectrum, MeOH, λ_{max}/nm, ε/L mol^{-1} cm^{-1}: [10^{-3} M] 585 s, br (3.2×10^2); [10^{-4} M] 430 br (2.81×10^4), 347 s (3.63×10^4), 331 m (4.42×10^4), 265 s (0.9×10^4). Fluorescence spectrum: (λ^{em}_{max} = 380, 400 nm; λ^{ex}_{max} = 355 nm). ESI mass data: calcd for $C_{27}H_{21}CuN_5O_2S$, $[M]^+$, $m/z = 542$; obsd. $m/z = 543$ s.

*4.2.7. [Cu(κ^3-O,N,S-L^4)(κ^2-N,N-bipy)] (**7**)*

To a suspension of [Cu^{II}(O,N,S-L^4] (0.027 g, 0.098 mmol) in a mixture of acetonitrile and methanol (1:1 v/v) was added solid bipy (0.015 g, 0.098 mmol) and the contents were stirred for 15 min. A clear dark green solution formed was allowed to evaporate at room temperature which yielded dark green complex (Yield. 0.036 g,

Table 2
Bond distances (Å) and bond angles (°) in complexes **1**–**5, 7, 8**.

[Cu(κ^3-O,N,S-L)(κ^2-N,N-bipy)] (**1, 3, 5** and **7**). ax = axial; eq = equatorial				
	1	**3**	**5**	**7**
Cu–O	1.9466(12)	1.9307(17)	1.9293(2)	1.913(3)
Cu–N	1.9522(13)	1.9567(18)	1.9529(14)	1.949(3)
Cu–S	2.2695(5)	2.2584(7)	2.2623(5)	2.2849(11)
Cu–N_{eq}	2.0192(13)	2.0451(19)	2.0274(15)	2.028(3)
Cu–N_{ax}	2.2529(14)	2.234(2)	2.253(15)	2.268(3)
O–Cu–N	93.43(5)	93.88(7)	92.63(6)	92.53(11)
N–Cu–S	85.31(4)	85.26(6)	85.61(4)	85.25(9
O–Cu–S	159.37(4)	160.47(6)	157.75(4)	161.62(11)
N–Cu–N_{eq}	177.28(6)	176.88(8)	179.22(6)	177.25(12)
N_{eq}–Cu–N_{ax}	76.59(5)	76.77(8)	76.32(6)	76.32(11)
τ value	0.298	0.273	0.357	0.260

[Cu(κ^3-O,N,S-L)(κ^2-N,N-phen)] (**2, 4** and **8**).				
	2		**4**	**8**
	2a	**2b**		
Cu–O	1.9466(12)	1.923(3)	1.9307(17)	1.9293(2)
Cu–N	1.958(3)	1.951(3)	1.9567(18)	1.946(3)
Cu–S	2.2611(10)	2.2740(11)	2.2584(7)	2.2790(12)
Cu–N_{eq}	2.031(3)	2.027(3)	2.0451(19)	2.037(3)
Cu–N_{ax}	2.276(3)	2.327(3)	2.234(2)	2.278(4)
O–Cu–N	92.26(11)	92.84(12)	93.83(10)	93.15(13)
N–Cu–S	85.31(9)	86.23(11)	85.30(8)	85.29(10)
O–Cu–S	153.33(9)	161.66(10)	159.68(8)	161.62(11)
N–Cu–N_{ax}	173.74(12)	176.43(13)	176.44(12)	77.38(15)
N_{eq}–Cu–N_{ax}	77.87(11)	76.65(12)	77.34(10)	176.24(15)
τ value	0.341	0.246	0.279	0.243

85%, M.p. 199–201 °C). μ_{eff} = 1.81 BM. $C_{19}H_{17}CuN_5O_2S$: Calcd. C 51.52; H 3.87; N 15.81; S 7.24; Found: C 51.36; H 3.63; N 16.03; S 6.95%. **IR** (KBr, selected absorption bands: ν(N^1–H) 3347 s, 3280 s (NH_2); ν(C–H) 3158 m, 3108 m, 3073 m, 2991 br, 2951 s, 2927 s; ν(C–H) 2831 m (CH_3O–); ν(C=N) + ν(C=C) + δ(N–H) 1626 s, 1586 s, 1533 s; δ(C–H) 1485 s, 1469 s,, 1458 s, 1438 s, 1415 s; 1302 s, 1250 s, 1215 s, 1192 s, 1044 s, 946 s, 836 s; ν(C–S) 816 s; 800 s, 769 s, 735 s, 704 s, 650 s, 627 s, 485 m cm^{-1}. Electronic absorption spectrum, MeOH, λ_{max}/nm, ε/L mol^{-1} cm^{-1}: [10^{-3} M] 580 br (2.0×10^2); [10^{-4} M] 389 s, br (6.10×10^3), 305 s (1.30×10^4), 287 m (1.41×10^4), 270 m (1.93×10^4). The crystals were grown from dichloromethane–methanol mixture (3:1 v:v). ESI mass data: calcd for $C_{19}H_{17}CuN_5O_2S$, $[M]^+$, m/z = 442; obsd. m/z = 443 s.

4.2.8. [Cu(κ^3-O,N,S-L^4)(κ^2-N,N-phen)] (**8**)

To a suspension of [Cu^{II}(O,N,S-L^4)] (0.028 g, 1.02 mmol) in a mixture of acetonitrile and methanol (1:1 v/v) was added solid bipyridine (0.024 g, 1.02 mmol) and the contents were stirred for 15 min. A clear dark green solution formed was allowed to evaporate at room temperature which yielded dark green complex (Yield. 0.037 g, 80%, M.p. 190–192 °C). μ_{eff} = 1.94 BM. $C_{21}H_{17}CuN_5O_2S$: Calcd. C 54.01; H 3.67; N 15.00; S 6.87; Found: C 53.87; H 3.46; N 15.18; S 7.01%. IR (KBr, selected absorption bands): ν(N^1–H) 3347 s, 3289 s (NH_2); ν(C–H) 3161 m, ν 3108 m, ν 3072 m, ν 2989 br, ν(C–H) 2834 m (CH_3O-); ν(C=N) + ν(C=C) + δ(N–H) 1630 s, 1586 s, 1533 s, δ(C–H) 1493 s, 1469 s, 1424 s; 1319 s, 1299 s, 1252 s, 1217 s, 1191 s, 1040 s, 942 s, 864 s, 844 s; ν(C–S) 812 s, 769 s, 702 s, 638 s, 484 m cm^{-1}. Electronic absorption spectrum (10^{-3}/10^{-5} m in MeOH, λ_{max}/nm, ε/L mol^{-1} cm^{-1}: [10^{-3} M] 585 br (1.85×10^2), [10^{-3} M] 420 m, br (1.23×10^4), 343 s (1.61×10^4), 328 s (2.10×10^4), 282 m (3.91×10^4). The crystals were grown from dichloromethane–methanol mixture (3:1 v:v). Fluorescence spectrum: (λ^{em}_{max} = 400, 460 nm; λ^{ex} = 355 nm).

4.3. X-ray crystallography

A single crystal was mounted on a glass fiber and used for data collection with a Xcalibur, Eos, Gemini (**1**, **5**), and a Bruker Kapa – Apex (II) CCD diffractometer (**2**–**4, 7, 8**), equipped with graphite monochromated Mo-*Kα* (λ = 0.71073 Å). Crystal data were collected at 173 (2) (**5**), 295(2) (**1**, **2**), 296(2) (**3, 4, 7, 8**) K. For complexes **1** and **5** data were processed with CrysAlisPro CCD (data collection), CrysAlisPro RED (cell refinement, data reduction) [41]. The structure was solved by direct methods using the program SHELXS- 97, refined by full-matrix least-squares techniques against *F*V using SHELX-97 and molecular graphics from SHELXL [42]. For complexes **2**–**4, 7, 8** data were processed with Bruker Kapa – Apex(II) CCD and corrected for absorption using SADABS [43]. The structures were solved by direct methods using SIR-92 software [43] and refined by full-matrix least-squares method based on *F*V using the program using SHELX-97 [42]. Atomic scattering factors taken from "International Tables for Crystallography" [44]. The crystallographic data and important bond parameters of complexes **1**–**5, 7** and **8** are given in Tables 1 and 2, respectively.

4.4. Antimicrobial studies

4.4.1. Test organisms

The reference strains of bacteria and yeast, used for testing their sensitivity to complexes, were obtained from Microbial Type Culture Collection (MTCC), Institute of Microbial Technology (IMTECH), Chandigarh, India and the clinical isolate methicillin resistant *Staphylococcus aureus* (MRSA) was obtained from Post graduate Institute of Medical Education and Research, (PGIMER), Chandigarh, India. Reference strains used Gram positive bacteria, *S. aureus*

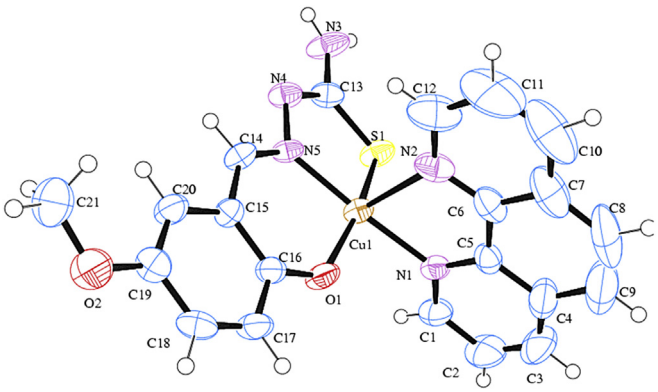

Fig. 7. Molecular structure of complex [Cu(κ^3-O,N,S-L^4)(κ^2-N,N-phen)] **(8).**

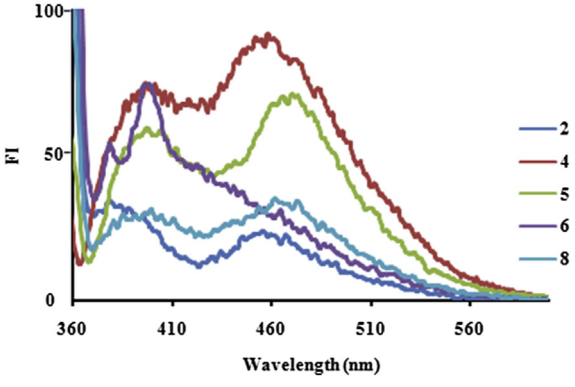

Fig. 8. Fluorescence spectral bands of complexes **2**, **4**–**6, 8**. {λ^{em}: (**2**) 378, 461; (**4**) 400, 456; (**5**) 400, 470; (**6**), 380, 400; (**8**) 400, 460 nm; λ^{ex} = 355 nm}.

Table 3
Biological data for complexes **1**–**8**.[a,b,c]

Complex/ligand	MRSA[e]	*S. aureus*[f]	*K. pneumoniae* 1[g]	*S. flexneri*[h]	*P. aeruginosa*[i]	*C. albicans*[j]
[Cu(L^1)(bipy)]**1**	25	27	26	N.A	N.A	31
[Cu(L^2)(bipy)]**3**	26	25	23	N.A	N.A	24
[Cu(L^3)(bipy)]**5**	27	25	26	15	17	23
[Cu(L^4)(bipy)]**7**	21	23	26	16	N.A	24
[Cu(L^1)(phen)]**2**	32	20	33	N.A	N.A	27
[Cu(L^2)(phen)]**4**	27	21	30	16	N.A	27
[Cu(L^3)(phen)]**6**	21	21	25	17	N.A	24
[Cu(L^4)(phen)]**8**	26	24	25	18	N.A	25
$[CuL^1]_n$[k]	20	15	20	N.A	N.A	15
$[CuL^2]_n$[k]	20	18	19	N.A	N.A	20
$[CuL^3]_n$[k]	17	17	20	N.A	12	21
$[CuL^4]_n$[k]	21	17	21	N.A	12	20
H_2L^1	N.A	14	12	N.A	N.A	12
H_2L^2	10	15	13	11	N.A	12
H_2L^3	17	15	14	11	N.A	15
H_2L^4	N.A.	15	10	N.A	N.A	14
Gentamycin[d,l]	N.A.	25[d]	32[d]	20[d]	17[d]	34[d]
Amphotericin[d,l]						

[a] All measurements are in mm diameter of the inhibition zone (N.A indicates no activity).
[b] The standard deviation varied in the range 0–1 based on three readings.
[c] Studies were made in dmso.
[d] Commercially available anti-microbial agents.
[e] Methicillin resistant *Staphylococcus aureus*.
[f] *Staphylococcus aureus*.
[g] *Klebsiella pneumoniae* 1.
[h] *Shigella flexneri*.
[i] *Pseudomonas aeruginosa*.
[j] *Candida albicans*.
[k] See Supporting information for more details of the compounds.
[l] Gentamycin acts as positive control against bacteria (*S. aureus*, *K. pneumoniae 1*, *S. flexneri*, *P. aeruginosa*) and Amphotericin acts as positive control against yeast (*Candida albicans*).

(MTCC740), Gram negative bacteria, *K. pneumoniae* 1 (MTCC109), *P. aeruginosa* (MTCC741), *S. flexneri* (MTCC1457) and one yeast strain *C. albicans* (MTCC227). The bacterial cultures were maintained on nutrient agar slants, and *C. albicans* was maintained on yeast malt agar.

4.4.2. Inoculum preparation

A loopful of isolated bacterial colonies and yeast colony were inoculated into 5 mL of respective medium and incubated at 37 °C and 25 °C respectively for 4 h. The turbidity of actively growing bacterial suspension was adjusted to match the turbidity standard of 0.5 Mc Farland units prepared by mixing 0.5 mL of 1.75% (w/v) barium chloride dihydrate ($BaCl_2 \cdot 2H_2O$) to 99.5 mL of 0.18 M (v/v) sulfuric acid with constant stirring. The microbial suspension so prepared was used for testing their sensitivity to all the compounds used.

4.4.3. Screening of compounds for antimicrobial activity by agar well diffusion assay

Sensitivity of different bacterial strains to different compounds was measured in terms of zone of inhibition using agar well diffusion assay [45]. All the compounds were dissolved in dimethyl sulfoxide (dmso) to a final concentration of 0.1%. The plates containing Muller Hinton agar medium, yeast malt agar and Sabouraud agar were spread with 50 μL of the bacterial and yeast inoculums respectively. Wells (6 mm diameter) were cut out from agar plates using sterilized stainless steel cork borer and filled with 50 μL of the compound. The plates were incubated at 37 °C and 25 °C for 24 h and diameter of resultant zone of inhibition was measured. Experiments were run in duplicate for each combination of extract and microbial strains. The results were compared with control in which compounds were replaced with dmso. In order to compare the effectiveness of compounds their activities were compared with standard antibiotic, namely, Gentamycin (1 mg/mL) for bacterial culture and amphotericin (1 mg/mL) for yeast culture. Gentamycin acts as positive control against bacteria (*S. aureus*, *K. pneumoniae 1*, *S. flexneri*, *P. aeruginosa*) and Amphotericin acts as positive control against yeast (*C. albicans*).

4.4.4. Minimum inhibitory concentration of complexes

Minimum inhibitory concentration (MIC) was worked out by agar dilution method. The compounds were prepared and

Table 4
Minimum Inhibitory concentration (MIC in μg/mL) of copper(II) complexes **1**–**8**.

Complex	MRSA	*S. aureus*	*K. pneumoniae* 1	*S. flexneri*	*P. aeruginosa*	*C. albicans*
[Cu(L^1)(bipy)]**1**	10 μg	10 μg	10 μg	–	–	5 μg
[Cu(L^1)(phen)]**2**	10 μg	25 μg	10 μg	–	–	5 μg
[Cu(L^2)(bipy)]**3**	10 μg	10 μg	25 μg	–	–	5 μg
[Cu(L^2)(phen)]**4**	5 μg	25 μg	5 μg	1000 μg	–	5 μg
[Cu(L^3)(bipy)]**5**	5 μg	10 μg	5 μg	1000 μg	750 μg	10 μg
[Cu(L^3)(phen)]**6**	25 μg	25 μg	10 μg	750 μg	–	10 μg
[Cu(L^4)(bipy)]**7**	25 μg	10 μg	5 μg	1000 μg	–	10 μg
[Cu(L^4)(phen)]**8**	5 μg	10 μg	10 μg	750 μg	–	10 μg

Methicillin resistant *Staphylococcus aureus* (MRSA), *Staphylococcus aureus* (*S. aureus*), *Klebsiella pneumoniae 1* (*K. pneumoniae* 1), *Shigella flexneri* (*S. flexneri*), *Pseudomonas aeruginosa* (*P. aeruginosa*), *Candida albicans* (*C. albicans*).

incorporated into Muller Hinton agar medium for bacteria and yeast malt extract medium for *C. albicans*. The plates were then inoculated with 25 μL of the activated bacterial and yeast strains by streaking with a sterile tooth pick and were further incubated at 37 °C for bacteria and 25 °C for yeast for 4 h and the lowest concentration of the extract causing complete inhibition of the bacterial growth was taken as MIC. The results were compared with that of control in which the sample was replaced with dmso. The experiment was performed in duplicate and repeated three times.

Acknowledgment

Financial assistance from UGC (BSR) and DST (X-ray diffractometer), New Delhi is gratefully acknowledged.

Appendix A. Supplementary data

Supplementary data related to this article can be found at http://dx.doi.org/10.1016/j.ejmech.2014.02.009.

References

[1] T.S. Lobana, R. Sharma, G. Bawa, S. Khanna, Coordination Chemistry Reviews 253 (2009) 977–1055.
[2] (a) S. Padhye, G.B. Kauffman, Coordination Chemistry Reviews 63 (1985) 127–160;
(b) D.X. West, S. Padhye, P.B. Sonawane, Structure and Bonding (Berlin) 76 (1991) 4–49;
(c) D.X. West, A.E. Liberta, S. Padhye, R.C. Chilkate, P.B. Sonawane, A.S. Kumbhar, R.G. Yerande, Coordination Chemistry Reviews 123 (1993) 49–71;
(d) J.S. Casas, M.S. Garcia-Tasende, J. Sordo, Coordination Chemistry Reviews 209 (2000) 197–261;
(e) J.S. Casas, M.S. Garcia-Tasende, J. Sordo, Coordination Chemistry Reviews 193 (1999) 283–359.
[3] (a) R.K. Mahajan, T.P.S. Walia, Sumanjit, T.S. Lobana, Analytical Sciences 22 (2006) 389–392;
(b) R.K. Mahajan, I. Kaur, T.S. Lobana, Talanta 59 (2003) 101–105;
(c) R.K. Mahajan, T.P.S. Walia, Sumanjit, T.S. Lobana, Talanta 67 (2005) 755–759;
(d) R.K. Mahajan, R. Kaur, T.S. Lobana, Indian Journal of Chemistry –Section A 45 (2006) 639–642;
(e) R.K. Mahajan, R.K. Puri, G. Bawa, T.S. Lobana, Zeitschrift fur Anorganische und Allgemeine Chemie 634 (2008) 1626–1632;
(f) D. Nandni, T.S. Lobana, R.K. Mahajan, Analytical Letters 42 (2009) 2474–2484.
[4] (a) S.V. Kolotilov, O. Cador, S. Golhen, O. Shvets, V.G. Ilyin, V.V. Pavlishchuk, L. Ouahab, Inorganica Chimica Acta 360 (2007) 1883–1889;
(b) S. Datta, D.K. Seth, R.J. Butcher, S. Bhattach- arya, Inorganica Chimica Acta 377 (2011) 120–128;
(c) S. Datta, D.K. Seth, S. Gangopadhyay, P. Karmakar, S. Bhattacharya, Inorganica Chimica Acta 392 (2012) 118–130;
(d) R. Saswati, C. Dinda, S. Schmiesing, E. Sinn, Y.P. Patil, M. Nethaji, H.S. Evans, R. Acharyya, Polyhedron 50 (2013) 354–363.
[5] (a) R.L. Arrowsmith, P.A. Waghorn, M.W. Jones, A. Bauman, S.K. Brayshaw, Z. Hu, G. Kociok-Kohn, T.L. Mindt, R.M. Tyrrell, S.W. Botchway, J.R. Dilworth, S.I. Pascu, Dalton Transactions 40 (2011) 6238–6252;
(b) S.I. Pascu, P.A. Waghorn, B.W.C. Kennedy, R. Arrowsmith, S.R. Bayly, J.R. Dilworth, M. Christlieb, R.M. Tyrrell, J. Zhong, R.M. Kowalczyk, D. Collison, P.K. Aley, G.C. Churchill, F.I. Aigbirhio, Chemistry – An Asian Journal 5 (2010) 506–519;
(c) S.I. Pascu, P.A. Waghorn, T.D. Conry, B. Lin, H.M. Betts, J.R. Dilworth, R.B. Sim, G.C. Churchill, F.I. Aigbirhio, J.E. Warren, Dalton Transactions (2008) 2107–2110.
[6] (a) S.I. Pascu, P.A. Waghorn, T.D. Conry, H.M. Betts, J.R. Dilworth, G.C. Churchill, T. Pokrovska, M. Christlieb, F.I. Aigbirhio, J.E. Warren, Dalton Transactions (2007) 4988–4997;
(b) M. Christlieb, A.R. Cowley, J.R. Dilworth, P.S. Donnelly, B.M. Paterson, H.S.R. Struthers, J.M. White, Dalton Transactions (2007) 327–331.
[7] E.B. Seena, M.R.P. Kurup, Polyhedron 26 (2007) 829–836.
[8] L. Latheef, M.R.P. Kurup, Spectrochimica Acta 70 (2008) 86–93.
[9] V.I. Prisakar, V.I. Tsapkov, S.A. Buracheéva, M.S. Byrké, A.P. Gulya, The Journal of Pharmaceutical Sciences 39 (2005) 30–32.
[10] M.B. Ferrari, S. Capacchi, G. Pelosi, G. Reffo, P. Tarasconi, R. Albertini, S. Pinelli, P. Lunghi, Inorganica Chimica Acta 286 (1999) 134–141.
[11] B.G. Patil, B.R. Havinale, J.M. Shallom, M.P. Chitnis, Journal of Inorganic Biochemistry 36 (1989) 107–113.
[12] P. Bindu, M.R.P. Kurup, T.R. Satyakeerty, Polyhedron 18 (1999) 321–331.
[13] A.D. Naik, P.A.N. Reddy, M. Nethaji, A.R. Chakravarty, Inorganica Chimica Acta 349 (2003) 149–159.
[14] A.M. Thomas, A.D. Naik, M. Nethaji, A.R. Chakravarty, Inorganica Chimica Acta 357 (2004) 2315–2323.
[15] R.P. John, A. Sreekanth, V. Rajakannan, T.A. Ajith, M.R.P. Kurup, Polyhedron 23 (2004) 2549–2559.
[16] T.S. Lobana, P. Kumari, R.J. Butcher, J.P. Jasinski, J.A. Golen, Zeitschrift fur Anorganische und Allgemeine Chemie 638 (2012) 1861–1867.
[17] D.X. West, M.M. Salberg, G.A. Bain, A.E. Liberta, Transition Metal Chemistry 21 (1996) 206–212.
[18] P. Ambalavanan, K. Palani, M.N. Ponnuswamy, Crystal Research and Technology 37 (2002) 1249–1254.
[19] D.X. West, Y. Yang, T.L. Klein, K.I. Goldberg, A.E. Liberta, J.V. Martinez, R.A. Toscano, Polyhedron 14 (1995) 1681–1693.
[20] E. Labisbal, K.D. Haslow, A.S. Pedrares, J.V. Martinez, S.H. Ortega, D.X. West, Polyhedron 22 (2003) 2831–2837.
[21] D.X. West, M.M. Salberg, G.A. Bain, A.E. Liberta, Transition Metal Chemistry 22 (1997) 180–184.
[22] G.A.A. Al-Hazmi, M.S. El-Shahawi, I.M. Gabr, A.A. El-Asmy, Journal of Coordination Chemistry 58 (2005) 713–733.
[23] J.V. Martinez, R.A. Toscano, A.Z. Dehesa, M.M. Salberg, G.A. Bain, D.X. West, Polyhedron 15 (1996) 427–431.
[24] T.S. Lobana, S. Khanna, G. Hundal, P. Kaur, B. Thakur, S. Attri, R.J. Butcher, Polyhedron 28 (2009) 1583–1593.
[25] T.S. Lobana, P. Kumari, G. Hundal, R.J. Butcher, Polyhedron 29 (2010) 1130–1136.
[26] T.S. Lobana, P. kumari, I. kaur, N. kaur, G. Garg, R.J. butcher, Journal of Coordination Chemistry 65 (2012) 1750–1764.
[27] (a) T.S. Lobana, P. Kumari, G. Hundal, R.J. Butcher, A. Castineiras, T. Akitsu, Inorganica Chimica Acta 394 (2013) 605–615;
(b) T.S. Lobana, P. Kumari, A. Castineiras, R.J. Butcher, European Journal of Inorganic Chemistry (2013) 3557–3566.
[28] H. Nikaido, Journal of Bacteriology 178 (1996) 5853–5859.
[29] M.J. Kuehnert, H.A. Hill, B.A. Kupronis, Emerging Infectious Diseases 11 (2005) 868–872.
[30] B.W. Frazee, J. Lynn, E.D. Charlebois, L. Lambert, D. Lowery, F. Perdreau-Remington, Annals of Emergency Medicine 45 (2005) 311–320.
[31] O. Azeez-Akande, African Journal of Clinical and Experimental Microbiology 11 (2010) 150–158.
[32] V.T. Trang, H. Takeuchi, H. Kudo, S. Katsuno, T. Shimamura, T. Kashiwagi, V.H. Son, T. Sugiura, H. Ukeda, Journal of Agricultural and Food Chemistry 59 (2011) 8953–8960.
[33] J. Zhang, Review of Bioinformatics & Biometrics (Rbb) (2013) 1–5.
[34] M.A. Ibrahim, A.A. Mansoor, A. Gross, M.K. Ashfaq, M. Jacob, S.I. Khan, M.T. Hamann, Journal of Nature Products 72 (2009) 2141–2144.
[35] H.Y. Kim, J.A. Wiles, Q. Wang, G.C.G. Pais, E. Lucien, A. Hashimoto, D.M. Nelson, J.A. Thanassi, S.D. Podos, M. Deshpande, M.J. Pucci, B.J. Bradbury, Journal of Medicinal Chemistry 54 (2011) 3268–3282.
[36] R.G. Finch, G.M. Eliopoulos, Journal of Antimicrobial Chemotherapy 55 (2005) 5.
[37] M.P. Pereira, S.O. Kelley, Journal of the American Chemical Society 133 (2011) 3260–3263.
[38] M.N. Alekshun, S.B. Levy, Cell 128 (2007) 1037–1050.
[39] (a) N.A. Berger, E.S. Johnson, A.M. Skinner Sr., Experimental Cell Research 96 (1975) 145–155;
(b) K.H. Falchuk, A. Krishan, Cancer Research 37 (1977) 2050–2056.
[40] T.S. Lobana, A. Sánchez, J.S. Casas, A. Castiñeíras, J. Sordo, M.S.G. Tasende, E.M.V. López, Journal of the Chemical Society, Dalton Transactions (1997) 4289–4299.
[41] Oxford Diffraction, CrysAlisPro CCD and CrysAlisPro RED, Oxford Diffraction Ltd, Yarnton, England, 2009.
[42] G.M. Sheldrick, Acta Crystallographica Section A 64 (2008) 112–122.
[43] A. Altomare, G. Cascarano, C. Giacovazzo, A. Guagliardi, Journal of Applied Crystallography 26 (1993) 343–350.
[44] A.J.C. Wilson, International Tables for Crystallography, vol. C, Kluwer Academic Publishers, Dordrecht, The Netherlands, 1995.
[45] A.W. Bauer, W.M.M. Kirby, J.C. Sherris, M. Turck, American Journal of Clinical Pathology 43 (1966) 493–496.